Excited levels in the multishaped ^{117}Pd nucleus studied via β decay of ^{117}Rh

J. Kurpeta,[1] A. Płochocki,[1] W. Urban,[1] T. Eronen,[2] A. Jokinen,[2] A. Kankainen,[2] V. S. Kolhinen,[3] I. D. Moore,[2] H. Penttilä,[2]
M. Pomorski,[1] S. Rinta-Antila,[2] T. Rząca-Urban,[1] and J. Wiśniewski[1]

[1]*Faculty of Physics, University of Warsaw, ul. Pasteura 5, PL-02-093 Warsaw, Poland*
[2]*Department of Physics, University of Jyväskylä, P.O. Box. 35, FIN-40351, Jyväskylä, Finland*
[3]*Cyclotron Institute, Texas A&M University, 3366 TAMU, College Station, Texas 77843-3366, USA*

Monoisotopic samples of exotic, neutron-rich ^{117}Rh nuclei, produced in the proton-induced fission of ^{238}U
and separated using the IGISOL mass separator coupled to the JYFLTRAP Penning trap, were used to perform
β and γ coincidence spectroscopy of ^{117}Pd. The spin parity of the ground state of ^{117}Pd was determined to be
$1/2^+$ and the 19.1 ms isomer at 203.2 keV was assigned a spin-parity $7/2^-$. The ^{117}Rh β^--decay scheme was
considerably extended, and various sequences of the levels were interpreted as resulting from the prolate, oblate,
and triaxial nuclear shapes. Some of the β^- decays were considered as the allowed Gamow-Teller transitions.
The experimental distribution of Gamow-Teller strength is discussed.

I. INTRODUCTION

The neutron-rich nucleus $^{117}_{45}$Rh with $N = 72$ has 14 neutrons more than the only stable isotope of rhodium, ^{103}Rh. The levels and transitions in ^{117}Pd, populated in the β^- decay of ^{117}Rh, currently represents the most rich spectroscopy information at the neutron-rich side of the $A = 117$ isobaric chain. In the next more exotic nucleus ^{117}Rh, there is only one excited level known, a submicrosecond isomer, which decays by a single γ ray of 321 keV [1].

A strong motivation for studies of these exotic nuclei is the longstanding prediction of a shape change from prolate to oblate deformation expected in this region [2,3]. The first experimental signs of this change were reported in ^{110}Mo [4] and ^{111}Tc [5,6]. In ^{111}Tc it was the observation of many extra low-energy excitations, as compared to lighter Tc isotopes, which was the sign of the occurrence of an oblate minimum in the nuclear potential. In the chain of Pd isotopes a hint of a transition to the oblate regime was recently reported in ^{115}Pd [7] in connection with the new spin-parity assignment of $1/2^+$ to the ground state (g.s.) and of $7/2^-$ to the isomer in this nucleus [6,8,9]. Therefore, the extension of these studies to ^{117}Pd is a natural step towards the identification of an oblate deformation, which is still a rare phenomenon in nuclei.

That some shape changes may occur in the Pd isotopes was already suggested by the extraordinary changes in the hindrance factors of isomeric transitions in $^{103-117}$Pd isotopes, which vary more than four orders of magnitude [10–13]. In these early works, it was assumed that in all these Pd isotopes spins of isomeric levels were $11/2^-$, corresponding to the spherical $\nu h_{11/2}$ excitation. Subsequent changes of some of these assignments [5,6,9] have shed new light on the effect. It is of interest to check whether any further changes in spin-parity assignments should be made in these isotopes, especially in ^{117}Pd.

Theoretical calculations support such expectations. In Ref. [2] Skalski *et al.* pointed to strong shape variations due to

the predicted coexistence of prolate and oblate potential minima and a γ softness expected in Mo-Pd nuclei. Many examples of these phenomena have been observed experimentally in the $100 < A < 120$ region, especially effects related to γ softness and triaxiality in neutron-rich Mo-Pd isotopes [4–10,14–29].

In the same region of the nuclide chart, calculations by Xu *et al.* [3] have described the evolution of nuclear deformation with an increasing neutron number from prolate through triaxial to oblate, predicting stability for oblate shapes at $N \geqslant 70$. New data for the exotic ^{117}Pd nucleus would provide an important and demanding case for testing such nuclear-model prediction far from stability.

This paper reports on the experimental investigations of excited levels in ^{117}Pd, populated in the β^- decay of ^{117}Rh and aimed at the verification of spins and parities of the ground state and the isomer in ^{117}Pd, as well as searching for new low-energy levels—the expected signature of an oblate deformation. In Sec. II we describe the experimental and analysis techniques used and the measurement performed in this work. Experimental results are presented in Sec. III. These results are discussed in Sec. IV, followed by more general discussion of Pd isotopes in Sec. V. Finally β-decay strength is discussed in Sec. VI and a summary is in Sec. VII.

II. EXPERIMENT

The ^{117}Rh nuclei were produced in fission of a natural uranium target, induced by 25 MeV protons from the K-130 cyclotron at the Accelerator Laboratory of the University of Jyväskylä. Fission products were on-line mass separated with the upgraded IGISOL-4 mass separator. The isobaric beam of 1^+ ions from the IGISOL [30], formed into bunches in a radio frequency cooler and buncher [31], was sent to the JYFLTRAP Penning trap for isobaric purification [32,33]. Figure 1 shows the spectrum of ions with mass $A = 117$ measured after the Penning trap using a microchannel plate (MCP) detector. The
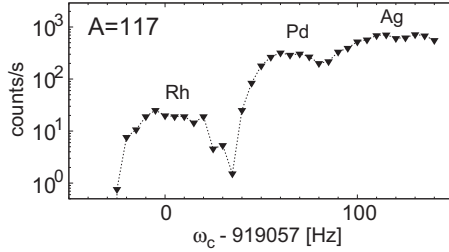
FIG. 1. Ion counts registered with a MCP detector placed after the Penning trap. The resolved atomic ions from the IGISOL isobaric beam are marked with their element symbols.

measurement was done as a function of the cyclotron frequency of ions inside the trap, $\omega_c = q \times B/m$, where q and m are the charge and mass of an ion and B is the magnetic field inside the trap. As seen in Fig. 1, JYFLTRAP can deliver a monoisotopic beam of ^{117}Rh. The rate of ^{117}Rh ions measured with the MCP detector was about 40 ions/s. The trap purification cycle was 131 ms.

The ^{117}Rh ions, released from the trap, were implanted into a movable plastic tape. The tape was moved every 5 s to transport away the long-lived, isobaric decay products. Our detector setup consisted of a 2 mm thick plastic scintillator and three low-energy germanium (LEGe) detectors equipped with thin (0.6 mm) composite carbon entrance windows to provide high transmission at low energy. The scintillation detector surrounding the implantation point was used for detecting electrons from β decay. In the vacuum chamber, containing the movable tape and the scintillation detector, there were three thin capton windows to minimize absorption of low-energy γ rays. The three LEGe detectors were arranged at 90° to each other in a horizontal plane around the vacuum chamber, each detector was facing one of the thin windows of the chamber. Average absolute efficiency of the LEGe detectors was about 4% at 100 keV and about 0.8% at 1000 keV.

A short measurement with the purification trap set to ^{117}Pd was made as well. It shows γ lines in the $A = 117$ decay chain, except for those populated directly in the ^{117}Rh decay, helping to identify new lines following β^- decay of ^{117}Rh. The β decay of ^{117}Pd monoisotopic samples was measured with the same setup as used for the β decay of ^{117}Rh.

The data acquisition system, based on the digital gamma finder (DGF) modules, was recording data from all the detectors in a triggerless mode. Later off line, data were time ordered and sorted into one- and two-dimensional coincidence histograms for further analysis.

III. β DECAY OF ^{117}Rh TO ^{117}Pd

The β decay of the neutron-rich isotope ^{117}Rh was for the first time observed in proton-induced fission of ^{nat}U. A β half-life of 0.44(4) s was measured and three γ rays of 34.6, 131.7, and 481.6 keV were ascribed to the decay of ^{117}Rh [10]. Later a similar β-decay half-life of 394^{+47}_{-43} ms was reported for ^{117}Rh produced by the fragmentation of a ^{136}Xe beam [34]. In the present work the coincidence between β particles, KX characteristic radiation and γ photons as well as double
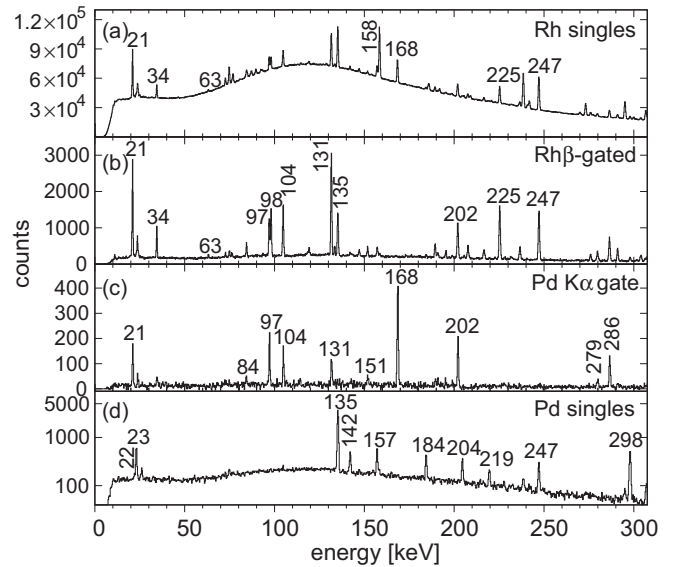

FIG. 2. The singles, β- and Pd($K_\alpha X$)-gated spectra measured with the LEGe detectors for the monoisotopic samples of ^{117}Rh (a)–(c) and monoisotopic samples of ^{117}Pd [(d), log. scale]. The peaks are labeled with their energies in keV.

γ coincidences were used to deduce the relations among γ transitions following the β decay of ^{117}Rh.

Examples of γ spectra recorded with the LEGe detectors are presented in Fig. 2. In Fig. 2(a) a spectrum from the ^{117}Rh monoisotopic samples shows all the recorded events with no additional conditions, the so-called singles spectrum. The spectrum in Fig. 2(b) shows all γ events, which are in coincidence with β events registered in the plastic scintillator. The β coincidence condition enhances γ lines emitted from excited levels populated by β decay and suppresses other γ lines, such as background radiation or isomeric transitions, compare spectra in Figs. 2(a) and 2(b). The spectrum in Fig. 2(c) shows γ lines in coincidence with the characteristic K_α radiation of palladium, thus one can see transitions between the excited states in ^{117}Pd. Finally, Fig. 2(d) shows a γ spectrum for the monoisotopic samples of ^{117}Pd, which is one step closer to the β stability valley than ^{117}Rh. Comparing Figs. 2(a) and 2(d) one may identify γ lines belonging solely to the ^{117}Rh β decay, which are present only in Fig. 2(a).

Figure 3 shows the quality of our coincidence spectra gated on lines of ^{117}Pd. The spectrum in Fig. 3(d) indicates the presence of the 17.8-keV link between the 207.7-keV and 225.4-keV levels.

Energies, intensities and coincidence relations for γ rays measured in this work are presented in Table I. The intensities of γ lines, visible in singles spectrum, were estimated based on peak areas in a spectrum recorded with the LEGe detector located opposite to the beam. The other two LEGe detectors were looking at the implantation point through a thin metal plates, which are used to support the plastic collection tape, thus their detection efficiency was reduced at low energies. For the γ lines not visible in the singles spectrum, their intensities were estimated using coincidence spectra. The β
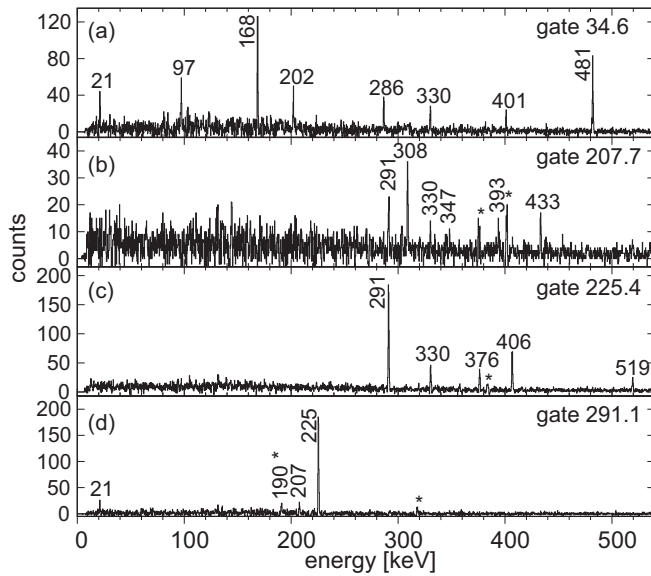
FIG. 3. The coincidence spectra for monoisotopic samples of ^{117}Rh. Energy of a gating γ line is shown in the top right corner. The peaks are labeled with their energies in keV and the ones due to backscattering are labeled with an asterisk.

feeding intensities to levels in ^{117}Pd populated via β decay of ^{117}Rh and the resulting $\log_{10} ft$ values are shown in Table II.

IV. EXCITED LEVELS IN ^{117}Pd

Using the coincidence relations shown in Table I, the β-decay scheme of ^{117}Rh was constructed and is presented in Fig. 4. The energy of ^{117}Rh β decay is as high as $Q_\beta = 7527$ keV [35]. Due to the low count rate of the very exotic nuclei, the contribution of naturally occurring γ radiation was significant. The γ spectra were recorded in a limited energy range because efficiency of a germanium detector decreases with increasing γ-ray energy. Therefore, some transitions of low intensity (especially at high γ energies) may have escaped detection. Consequently the β feeding values observed in this work, which are shown in Table II, must be considered as upper limits and the corresponding $\log_{10} ft$ values as lower limits.

A. Spin parity of the ^{117}Rh ground state

The knowledge of the spin parity of the ground state of ^{117}Rh is of prime importance for assigning spins and parities to levels in ^{117}Pd, populated in the β decay of ^{117}Rh. An axially asymmetric deformation is proposed for rhodium isotopes to explain the nuclear structure observed in spectroscopy measurements [1,38,39]. Theoretical calculations of the potential-energy surface for ^{117}Rh, based on the FRLDM macroscopic-microscopic model, show a single minimum for the axial-asymmetry coordinate $\gamma \approx 45°$ [40].

The lowest states in neutron-rich rhodium isotopes can be explained using the scheme of proton single-particle levels calculated as function of an axial asymmetry γ for a quadrupole deformation fixed at $\beta = 0.31$ [41]. The calculations suggest $7/2^+$ spin assignments for ground states in $^{105-115}$Rh.

These expectations can be verified further by observing systematic trends of experimental excitations. Examples of such systematics for odd-mass rhodium isotopes can be found in Refs. [1,27]. In Fig. 5 we show an updated version, displaying experimental excitation energies of some characteristic levels in odd-A isotopes of rhodium. Levels are drawn relative to the $9/2^+$ excitation, which in spherical Rh isotopes is most likely dominated by the $\pi g_{9/2}$ configuration.

The $1/2^-$ excitation corresponding to the ground state in spherical ^{101}Rh, is due to the $\pi p_{1/2}$ configuration. Its energy increases quickly with deformation (neutron number), in accord with Nilsson scheme predictions for the $1/2^-$[301] orbital, and is not expected to play any role at low excitations in ^{115,117}Rh. Similarly, the $1/2^+$ level, corresponding to the $1/2^+$[431] intruder orbital, departs quickly from the $9/2^+$ excitation past ^{109}Rh and should be well above the ground state in ^{115,117}Rh. Its minimum energy in ^{109}Rh suggests the maximum deformation in Rh isotopes at the neutron number $N = 64$, i.e., around the middle of the $50 < N < 82$ shell.

Only in the spherical ^{101}Rh the $7/2^+$ level lies above the $9/2^+$ level. The ground-state levels of all known Rh isotopes from ^{105}Rh up have spin parity $7/2^+$. As pointed out in Ref. [52] in isotopes with some collectivity this excitation is most probably due to seniority-three coupling of protons occupying the $\pi g_{9/2}$ shell. Therefore, one may expect the $7/2^+$ level below the $9/2^+$ level in Rh isotopes with N in the region 58–64.

The systematics in Fig. 5 suggests that above neutron number $N = 68$ (^{113}Rh) the $7/2^+$ level rises, which may be due to lowering of collectivity above the midshell. This is supported by the systematics of $3/2^+$ and $11/2^+$ levels shown in Fig. 5, which can be interpreted as the antiparallel and parallel, $7/2^+ \otimes 2^+$ couplings, respectively, but from $N = 62$ these states form regular bands based on a triaxial ground state and $3/2^+$ state [39,53,54]. We also note a rapid change at ^{119}Rh, though it should be remembered that these data are rather tentative [39]. In conclusion, the stable trend of $\pi(g^3_{9/2})_{j-1}$ $7/2^+$ levels shown in Fig. 5, points to preliminary $7/2^+$ spin-parity assignment for the ground state of ^{117}Rh.

It is of interest to find the reason for the suggested changes in collectivity (deformation) of Rh isotopes past $N = 68$. A possible cause could be a change from prolate to triaxial or oblate deformation in Rh isotopes, which is expected around this neutron number [2,3].

B. Levels related to the 19 ms isomer and the ground state of ^{117}Pd

The 203-keV isomeric level in ^{117}Pd with a half-life of 19.1 ms was reported in Refs. [11,55] and later in the discussion of the low-energy states populated by the ^{117}Rh β^- decay [10,12]. Five transitions of energies 34, 71, 97, 131, and 168 keV were ascribed to the decay of the isomer. The 71 and 168 keV transitions, depopulating the isomeric level, were assigned a $M2$ multipolarity based on the spectroscopy of conversion electrons. Using the systematics available at that time, $11/2^-$ spin was assigned to the isomer and the $7/2^+$, $7/2^+$, and $5/2^+$ spins were assigned to the 131-, 34-keV, and the ground state, respectively. The results of Refs. [10–12,55]

TABLE I. Energies, relative intensities I_γ, and coincidence relations of γ lines observed in the β^- decay of ^{117}Rh. [w]weak coincidence; [u]unplaced in the scheme; [Ag]also in Ag; [Cd]also in Cd; and [In]also in In.

E_γ (keV)		I_γ	from	to	coincident γ lines
17.8(4)		2.3(1.5)	225.4	207.7	207[w]
34.6(1)		55.6(2.0)	34.6	0.0	21, 97, 104, 168, 202, 286, 330, 401, 481, 567
63.3(3)		6.2(9)	266.5	203.2	
71.4(7)		1.3(4)	203.2	131.7	97, 131, 273[In]
84.6(1)		10(2)	321.3	236.7	21, 34[w], 97, 104, 131, 202, 236, 423
93.9(5)		2.4(4)	225.4	131.7	131
97.0(1)		34.9(1.6)	131.7	34.6	21, 23, 34, 84, 104, 189, 279, 307[w], 384, 412, 423, 469
104.9(1)		49.7(1.8)	236.7	131.7	21, 23, 84, 97, 131, 198, 279, 307, 390, 395, 507, 533, 601[u], 612
131.7(1)		100.0(1)	131.7	0.0	21, 23, 71, 84, 93, 104, 189, 195, 198, 279, 307, 384, 390, 395, 412, 423, 469, 533, 612, 628[u], 707[w]
151.9(3)		8.7(1.0)	516.5	364.7	21, 330
168.6(1)		91.7(6.0)	203.2	34.6	21, 23, 34
189.4(2)		18.0(1.8)	321.2	131.7	21, 97, 131, 195, 306, 423
190.9(8)		6.2(0.8)	225.4	34.6	21, 291, 330, 406
195.5(5)		7.7(1.0)	516.5	321.2	21, 131, 189, 286
198.9(3)		4.3(1.6)	435.6	236.7	21, 104, 131, 202, 236
202.1(1)	[Cd]	43.5(5.0)	236.7	34.6	21, 23, 34, 84, 198, 279, 307, 390, 395, 507, 533, 612
207.7(1)		18.9(2.0)	207.7	0.0	17[w], 21[w], 291, 308, 330, 348[w], 393, 406[w], 433, 519[w]
225.4(1)		80.3(2.8)	225.4	0.0	291, 330, 376, 406, 415, 519, 613, 808, 1689
228.1(1.9)		1.6(8)	744.6	516.5	481
236.7(1)		20.3(2.0)	236.7	0.0	84, 198, 279, 307, 390, 395
279.9(2)		18.4(1.2)	516.5	236.7	21, 97, 104, 131, 202, 236
286.6(1)		45.6(3.0)	321.2	34.6	21, 23, 34, 195, 306, 423
291.1(2)		23.8(2.0)	516.5	225.4	17[w], 21, 97, 207, 225
306.1(4)		5.3(1.5)	627.4	321.2	21, 131, 189, 286
307.7(2)	[Cd]	10(1.9)	544.4	236.7	21, 23, 97, 104, 131, 202, 236, 401
308.8(3)		2.9(0.7)	516.5	207.7	21, 34, 131, 202, 207, 401
308.8(3)		2.9(0.7)	744.6	435.6	21, 34, 131, 202, 207, 401
330.1(4)		35(5)	364.7	34.6	21, 23, 34, 151, 380, 473
330.6(9)		5.8(2.0)	555.6	225.4	191, 207, 225
334.5(7)		1.0(5)	770.0	435.6	401
348.2(7)		1.9(1.0)	555.6	207.7	207
376.3(5)		7.1(1.5)	601.7	225.4	21, 225
380.2(3)		7.0(1.2)	744.6	364.7	21, 330
384.5(4)		19.1(2.2)	516.5	131.7	21, 97, 131
390.8(3)		8.7(1.5)	627.4	236.7	21, 23, 97, 104, 131, 202, 236
393.9(4)		1.9(1.0)	601.7	207.7	
395.5(4)		5.8(2.0)	632.1	236.7	21, 34, 97, 104, 131, 202, 236
401.0(3)		28(3)	435.6	34.6	21, 23, 34, 308, 493, 587, 620[u]
406.7(2)		15.3(2.0)	632.1	225.4	225
412.9(3)		9.3(1.1)	544.4	131.7	21[w], 97, 131
415.4(8)		2.1(1.0)	641.0	225.4	21[w], 225
423.4(3)		5.8(2.0)	744.6	321.2	21, 34[w], 84, 97, 131, 286
423.8(3)		14.7(2.0)	555.6	131.7	21, 34[w], 84, 97, 131, 286
433.5(9)		3.9(1.5)	641.0	207.7	207
469.9(7)		8.7(1.5)	601.7	131.7	21[w], 23[w], 34, 97, 131
473.9(4)		3.5(1.5)	838.6	364.7	330
481.9(1)	[Ag]	133(10)	516.5	34.6	21, 23, 34, 147[Ag], 228

TABLE I. (*Continued.*)

E_γ (keV)		I_γ	from	to	coincident γ lines
493.7(1.0)		3.4(1.0)	929.3	435.6	401
507.7(8)		3.9(1.5)	744.6	236.7	104, 202
519.1(7)		5.5(1.5)	744.6	225.4	207$^{\mathrm{w}}$, 225
533.2(9)		4.4(1.0)	770.0	236.7	21, 97, 104, 131, 202
567.2(5)		15.6(3.0)	601.7	34.6	21, 34
587.6(1.7)	$^{\mathrm{Ag}}$	3.1(1.0)	1023.2	435.6	21, 401
612.3(9)		2.7(1.0)	849.0	236.7	21, 104, 131, 202, 225
612.7(7)		3.1(1.0)	744.6	131.7	21, 104, 131, 202, 225
613.2(6)		2.3(1.0)	838.6	225.4	21, 104, 131, 202, 225
707.0(1.5)		2.4(1.0)	838.6	131.7	131
808.1(1.5)		3.3(1.0)	1033.5	225.4	225
1689.1(1.2)		5.9(1.0)	1914.5	225.4	21, 225

summarized above, came from the simultaneous spectroscopy studies of all the neutron-rich nuclei in the $A = 117$ isobaric chain since the best mass resolving power of the available separation techniques was limited to select isobars, only. The production rate of the isomer in ^{117}Pd was estimated one order of magnitude higher than the production rate of ^{117}Rh [12].

The excited levels in ^{117}Pd, populated in the spontaneous fission of ^{248}Cm were investigated by prompt γ spectroscopy with the EUROGAM2 array [8]. A new γ transition of 63.3 keV was observed to feed the 203.2-keV isomeric. Consequently the $11/2^-$ spin parity was assigned to the 266.5-keV level and spin of the isomeric level was lowered to $9/2^-$. The 63.3 keV

TABLE II. β feeding intensities (I_β) and $\log_{10} ft$ values of excited levels populated in the β^- decay of ^{117}Rh. The I_β value to the 131.7-keV level is 0 or 4.6 for the $E2$ or $M1$ multipolarity of the 104.9 keV line, respectively. For some transitions in ^{117}Pd the multipolarities were deduced [12] and their total conversion coefficients were taken from Ref. [37]. Total intensity of 17.8 keV was estimated as 7(3) γ units. ^{117}Rh $T_{1/2} = 421(30)$ ms [36].

E_{lev} (keV)	I_β	$\log_{10} ft$	E_{lev} (keV)	I_β	$\log_{10} ft$
0.0	0.0		555.6	2.9(0.4)	6.0
34.6	0.1(2.1)	7.8	601.7	4.3(0.5)	5.9
131.7	0–4.6	$\geqslant 6.0$	627.4	1.8(0.3)	6.2
203.2	$\leqslant 19.2$ (1.2)	$\geqslant 5.3$	632.1	2.7(0.4)	6.0
207.7	0.0		641.0	0.8(0.2)	6.6
225.4	3.7(0.8)	6.0	744.6	3.4(0.4)	5.9
236.7	7.4(1.0)	5.7	770.0	0.7(0.1)	6.6
266.5	1.9(0.2)	6.3	838.6	1.0(0.3)	6.4
321.2	5.9(0.6)	5.8	849.0	0.3(0.1)	6.9
321.3	2.0(0.3)	6.3	929.3	0.4(0.1)	6.8
364.7	1.9(0.7)	6.3	1023.2	0.4(0.1)	6.8
435.6	3.2(0.5)	6.0	1033.5	0.4(0.1)	6.7
516.5	27.7(1.7)	5.1	1914.5	0.8(0.1)	6.2
544.4	2.5(0.3)	6.1			

transition in ^{117}Pd was confirmed in another study, using a ^{252}Cf spontaneous-fission source [9].

In this work, with the use of a Penning trap as a precise mass filter, monoisotopic samples of ^{117}Rh were studied. In the singles γ spectrum [see Fig. 2(a)] one observes, for the ion trap frequency set to ^{117}Rh, the 71.4- and 168.6-keV lines depopulating the isomer and the 63.3-keV line observed before in the spontaneous fission study [8,9]. The 63.3-keV line is not coincident with any other line in our β-decay data and this is why we think that it populates directly the 203.2-keV isomer. This leads to the conclusion that the 203.2- and 266.5-keV levels are populated (directly or indirectly) following β decay of ^{117}Rh. A considerable β feeding to the 203.2-keV level (see Table II) is an upper limit, in our coincidence data it was not possible to find any other γ transitions populating the isomer. The experimental $\log_{10} ft \geqslant 5.3$ can not exclude a singly forbidden β transition to the 203.2-keV level, as such forbidden transitions with $\log_{10} ft < 6$ are known in other nuclei.

Intensity balances for the 34.6- and 131.7-keV levels, shown in Table II, indicates they are not (or only weakly) populated in β decay. With the $7/2^+$ spin and parity for the ground state of ^{117}Rh and the $M2$ multipolarities of the 71- and 168-keV transitions [10] one may explain the observed β feeding to the low-energy levels in ^{117}Pd by assigning spin parity $9/2^-$ for the 266.5-keV level, $7/2^-$ to the 203.2-keV isomer and $3/2^+$ to the levels at 34.6 and 131.7 keV.

We note that the 203.2-keV isomer does not decay to the ground state. This suggests that the spin of the ground state is lower than $3/2$ or the structure of the ground state is significantly different from structures of the 34.6- and 131.7-keV levels. While this latter possibility needs further investigations, we note that the presence of prompt 34.6- and 131.7-keV transitions to the ground state does not favor very different structures. Therefore, we propose spin parity $1/2^+$ for the ground state of ^{117}Pd.

With the $1/2^+$ spin parity, the ground-state branching in the β decay of ^{117}Rh is assumed to vanish, correcting the 70% feeding proposed in Ref. [10], where $5/2^+$ spin parity was
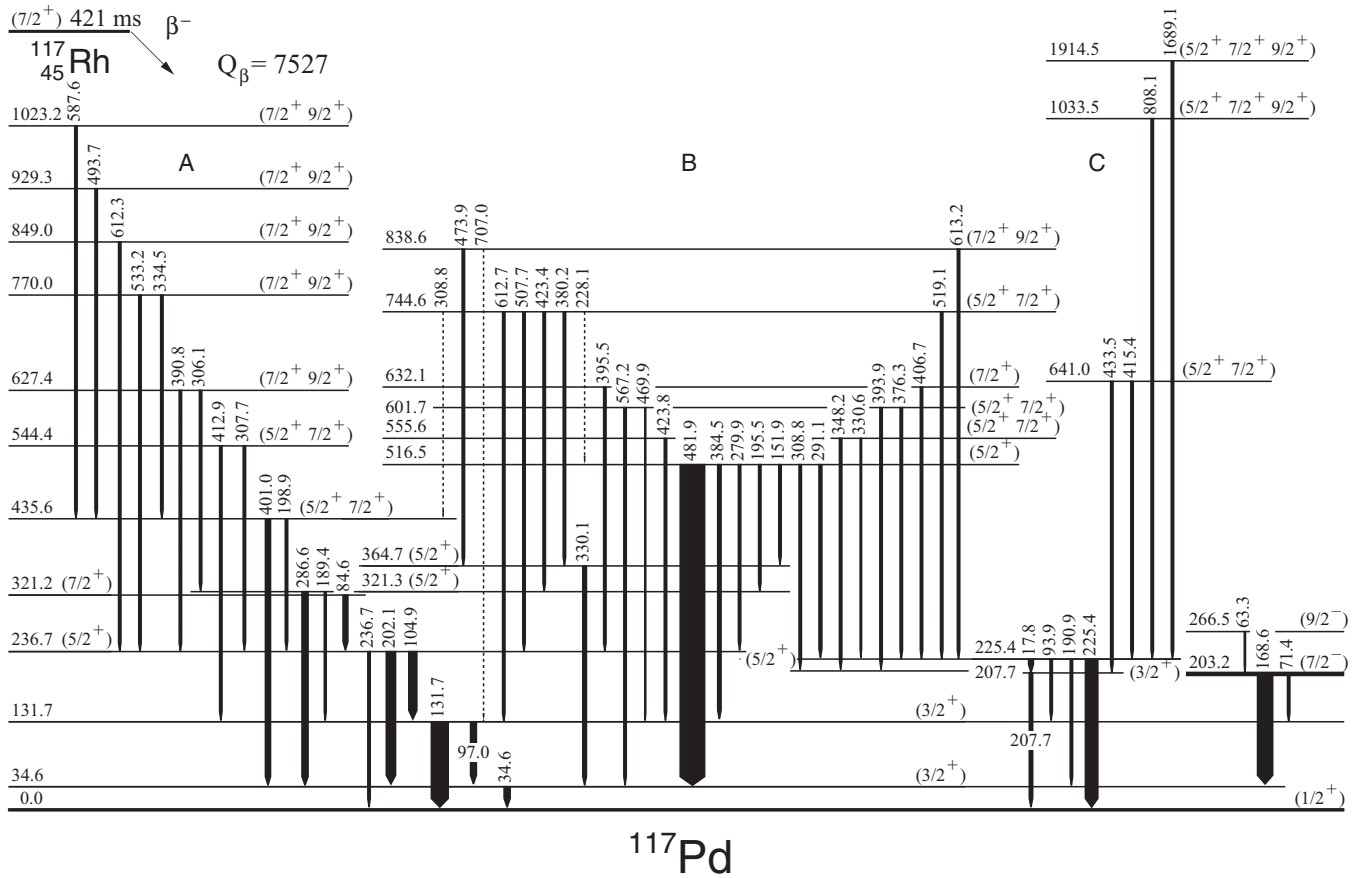
FIG. 4. Excitation scheme of ^{117}Pd as obtained in this work. We interpret the three groups of levels, marked A, B, and C, as related to prolate, triaxial, and oblate deformation, respectively. The Q_β in keV was taken from Ref. [35] and the half-life from Ref. [36].
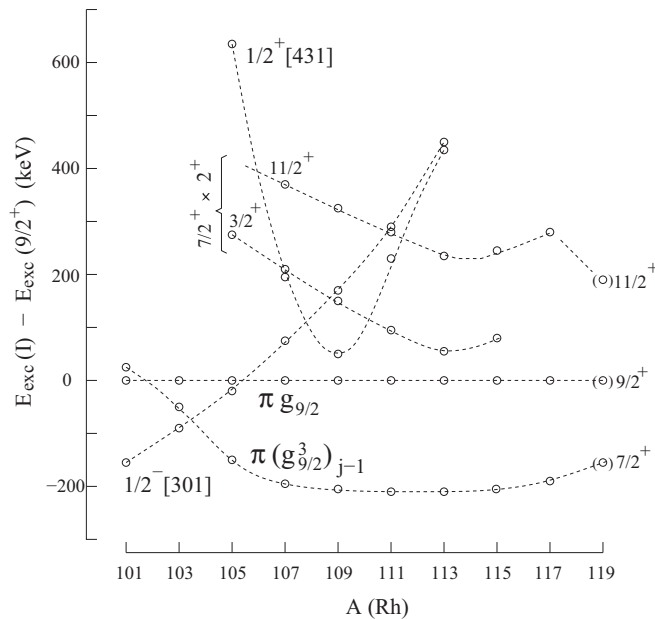

FIG. 5. Systematics of selected excited levels in odd-A Rh isotopes. The data are taken from Refs. [12,39,42–51]. Dashed lines are drawn to guide the eye.

assumed for the ground state of ^{117}Pd. It may be noted, that in our paper on β decay of ^{115}Rh [7], we assigned spin parity $7/2^-$ to the isomeric state in ^{115}Pd and changed spin of the ground state to $1/2^+$.

C. Levels 236.7 keV, 207.7, and 225.4 keV

There are three excited levels of similar energies 207.7, 225.4, and 236.7 keV, which exhibit significantly different decay properties. The 236.7-keV level is fed in β decay (7.4%) and deexcites by 104.9 ($M1$ 8.4-$E2$ 13.8%), 202.1 (5.5%). and 236.7 (2.6%) keV transitions, where % is given in β intensity units. It is the highest-energy level that deexcites directly to the ground state. Its feeding in β decay ($\log_{10} ft = 5.7$) and the observed γ-decay branchings point to its $5/2^+$ spin parity.

The 207.7-keV level, which is not populated in β decay, deexcites by the 207.7-keV (2.5%) transition to the ground state. The 225.4-keV level is populated in β decay ($\log_{10} ft = 6.0$) and deexcites by four transitions: 17.8 (0.9%), 93.9 (0.4%), 190.9 (0.8%), and 225.4 (10.7%) keV. The levels 207.7 and 225.4 keV are connected by the 17.8-keV transition not seen in the singles spectrum, but are well confirmed by the coincidence relations. Considering the β-decay feeding and γ deexcitation patterns, the most probable spins and parities for these levels are $3/2^+$ and $5/2^+$, respectively.
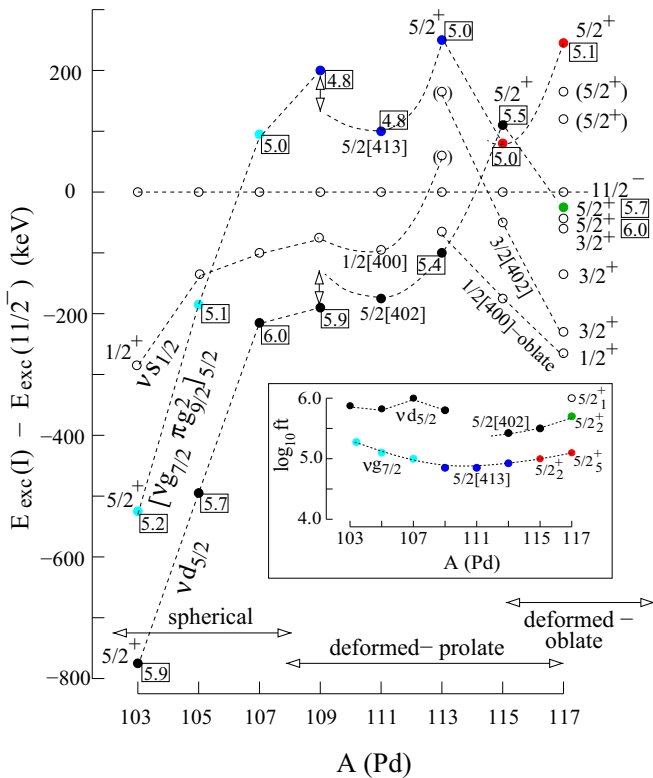
FIG. 6. Systematics of low-spin, positive-parity excited levels in odd-A Pd isotopes. The data are taken from Refs. [4,6,44–51] and the present work. Dashed lines are drawn to guide the eye.

D. 516.5-keV level

The 516.5-keV level has the highest population of 27.7% in β decay. It shows no relation to higher-lying levels, except a weak 228.1-keV line. The strongest line of 481.9 keV, depopulating this level, was already observed in Refs. [10,12] but was not placed in the decay scheme. Considering the $\log_{10} ft = 5.1$ of this level and its decay to $3/2^+$ level the spin parity of this level must be $5/2^+$ or $7/2^+$. Of the two spins $5/2^+$ is more likely as suggested by the systematics of 5/2 levels in the inset of Fig. 6 (red points). Somewhat puzzling is the lack of any decay of the 516.5 keV to the $1/2^+$ g.s.

E. Other excited levels in ^{117}Pd

The levels at 321.2, 321.3, 435.6, 544.4, 555.6, 601.7, 641.0, and 744.6 keV deexcite to the $3/2^+$ and $5/2^+$ states, thus their most probable spins are 5/2 and 7/2. The excited levels at 627.4, 632.1, 770.0, 838.6, 849.0, 929.3, 1033.5, and 1914.5 keV deexcite to the $5/2^+$ and $7/2^+$ states, thus their most probable spins are 7/2 and 9/2. The 321.2-keV level, which decays to the $5/2^+$ level at 236.7 keV only and is not populated from any other level, has most likely a spin parity $7/2^+$. The 321.3- and 364.7-keV levels, which decay to the $3/2^+$ levels only, both have, most likely, spin parity $5/2^+$. The levels at 435.6, 544.4, 555.6, 601.7, 641.0, and 744.6 keV, all with $\log_{10} ft$ values around 6.0 and deexciting to $3/2^+$ and $5/2^+$ states have spins $5/2^+$ or $7/2^+$. Excited levels at 627.4, 632.1,

770.0, 838.6, 849.0, 929.3, 1023.2, 1033.5, and 1914.5 keV, with $\log_{10} ft$ values around 6.5, deexciting to the $5/2^+$ and $7/2^+$ states, have probable spins of 5/2, 7/2 or 9/2.

V. DISCUSSION

With the total $\log_{10} ft \approx 4.5$, for β^- decay of the ground state of ^{117}Rh to the observed positive-parity levels in ^{117}Pd, this decay must involve the allowed Gamow-Teller transitions. In this section we will trace them and try to clarify other transitions. It is particularly important to explain the pronounced population of the negative-parity states in ^{117}Pd in the decay of ^{117}Rh. We will also discuss possible signatures of oblate or triaxial shape in Pd isotopes.

A. Positive-parity levels in Pd isotopes

The general structure of the positive-parity levels in lighter odd-A Pd isotopes was described in the recent study of ^{109}Pd [52]. Below, we present this picture updated with the new data for ^{117}Pd and some new observations for lighter Pd isotopes, which should help understanding the structure of ^{117}Pd observed in this work.

As can be seen in the Nilsson diagram the bone structure of the $^{103-115}$Pd isotopes is based on the interacting $5/2^+[413]$ and $5/2^+[402]$ orbitals, originating from the $d_{5/2}$ and $g_{7/2}$ neutron shells. In spherical ^{103,105}Pd isotopes the odd neutron occupies the $d_{5/2}$ shell, producing $5/2^+$ ground states. With the increasing neutron number the occupation moves to orbitals originating from the $g_{7/2}$ shell. However, the interaction of the two results in the $5/2^+[402]$ still having the properties ($\log_{10} ft$) characteristic of the $d_{5/2}$ shell. Therefore in a long chain from ^{103}Pd to ^{113}Pd the ground state has the same spin parity $5/2^+$ and similar properties. Figure 6 shows these levels (black circles, labeled $\nu d5/2$ and $5/2[402]$), drawn relative to the excitation stemming from the $1h_{11/2}$ orbital with the corresponding $\log_{10} ft$ values shown in rectangular boxes.

The $5/2_2^+$ excitation, expected at higher energy, starts in ^{103}Pd as the $g_{7/2}$ neutron coupled with a pair of $g_{9/2}$ protons to produce the $5/2^+$ $j-1$ anomalous state. At higher neutron number this evolves into the $5/2[413]$ orbital, which after virtual crossing with the $5/2[402]$ orbital retains the properties of the $\nu g_{7/2}$ shell. These excitations are shown in Fig. 6 as cyan and blue circles with $[\nu g_{7/2} \pi g_{9/2}^2]_{5/2}$ and $5/2[413]$ labels and with the corresponding $\log_{10} ft$ values in rectangular boxes.

We note that in ^{109}Pd, where the pseudocrossing takes place, the positions of $5/2_1$ and $5/2_2$ levels are displaced with respect to positions suggested by systematics for the $5/2[402]$ and $5/2[413]$ levels. This is probably due to the interaction between these two orbitals.

The $\log_{10} ft$ values in the rectangular boxes display regular trends, as shown in the inset of Fig. 6. The values for the ground states in $^{103-109}$Pd, ($\nu d_{5/2}$), which scatter around 5.9, suggest a hindered β decay, supporting a β transition from the $d_{5/2}$ neutron in the ground state of ^{117}Rh to the $g_{9/2}$ proton in ^{117}Pd. At higher neutron number, the two points for $5/2_1$ levels in ^{113,115}Pd (labeled $5/2[402]$) are a likely continuation of this trend. The $\log_{10} ft \approx 5.5$ for these two points is lower,
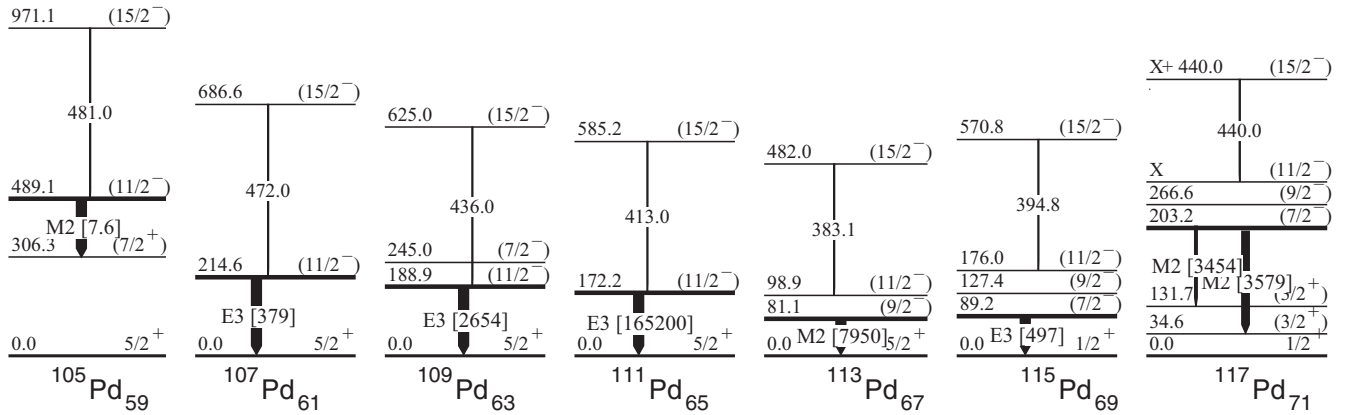
FIG. 7. Systematics of the isomeric states and transitions and other relevant levels in the odd-A Pd isotopes. The hindrance factors of the isomeric transitions are shown in square brackets, the factors for ^{117}Pd were calculated using intensities found in this work. The data are taken from Refs. [12,13,56], ENSDF and the present work.

probably due to the interaction with the $5/2_2$ levels. Until now the $\log_{10} ft$ for the ground state of ^{111}Pd has not been determined but assuming that this state also corresponds to the $\nu 5/2[402]$ configuration, its expected $\log_{10} ft$ is 5.4, which corresponds to 20% feeding in β decay to the ground state of ^{111}Pd. The $\log_{10} ft$ value for the $5/2_2$ level in ^{117}Pd (green point in the figure and in the inset, corresponding to the 236.7-keV level in ^{117}Pd) suggests that this level has similar structure though it does not continue the energy systematics.

The $\log_{10} ft$ values around 5.0 corresponding to the $5/2_2^+$ levels, indicate an allowed β decays to these levels. The allowed character of the transitions can be explained as the G-T transitions from the ground state of Rh isotope containing an admixture of a pair of $g_{7/2}$ neutrons, in which one of these neutrons is converted into the $g_{9/2}$ proton. This is observed from ^{103}Pd to ^{113}Pd in both, spherical and deformed nuclei.

The trend of $\log_{10} ft$ values for the $5/2_2$ levels, seen in the inset, suggests that the $5/2_2$ level in ^{115}Pd and the $5/2_5$ level in ^{117}Pd (red points), should also be populated by G-T transitions, i.e., should contain the $g_{7/2}$ neutron in their structure. However, the systematic trend of excitation energies of these $5/2_2$ levels in ^{115,117}Pd (red points in the main figure) does not match the trend of $5/2[413]$ excitations in $^{109-113}$Pd (blue points). Similar comments concern the 236.7-keV, $5/2_1$ level in ^{117}Pd (the green point). There are also two further observations (i) the quick lowering of $1/2^+$ and $3/2^+$ levels with increasing neutron number and (ii) the increase in a number of low-energy levels in ^{117}Pd, as compared to lighter isotopes.

All these effects observed in ^{117}Pd (and partly in ^{115}Pd) suggest that above the neutron number $N = 67$ there is a change in the structure of Pd isotopes. The possible explanation is the appearance of an extra minimum in the nuclear potential. This could explain the doubling of the number of low-energy excitations in ^{117}Pd. As expected theoretically [2,3] a new minimum corresponding to an oblate shape would appear at high neutron number. The details of the competition of both minima is a challenge for the future calculations. We note that the fact that, on the one hand the $5/2_1$ and $5/2_5$ levels in ^{117}Pd are similar in nature to the $5/2_1$ and $5/2_2$ levels in lighter

isotopes, while their excitation energies do not follow the trend, on the other hand, suggest an interaction between the prolate and the oblate minima in the potential.

B. Isomers and negative-parity levels in Pd isotopes

The assignment of spin parity $7/2^-$ to the 19.1 ms isomer in ^{117}Pd, proposed in this paper, is an important new result. Apart from providing, in turn, a new spin parity of $1/2^+$ to the ground state of ^{117}Pd, it may help understanding the very intriguing hindrance factors of isomeric transitions, which vary more than four orders of magnitude in neutron-rich palladium nuclei.

The decays of isomers in odd-A, $^{105-117}$Pd isotopes are collected in Fig. 7, showing the behavior of isomeric states and the levels associated with isomers. The properties of isomeric states in odd-A, neutron-rich palladium isotopes were reported in Refs. [12,13], among them the hindrance factors for isomeric transitions, shown in Fig. 7 in square brackets next to $M2$ or $E3$ labels of isomeric transitions.

The hindrance factor of 7.6, for the isomeric transition in ^{105}Pd is typical for an $M2$ transition between single-particle levels in a spherical nucleus (cf. the compilation [57] and the hindrance factors of 11 and 8 for $M2$-$E3$ transitions in ^{109}Cd and ^{103}Ru). It is the huge increase to the 165 200 hindrance in ^{111}Pd, which is puzzling. The authors of Refs. [12,13] proposed differences in pairing but pointed out that this can not be the only reason and suggested different shapes of the involved nuclear levels.

In transitional nuclei excited levels originating from high-j intruder orbitals can maintain their almost single-particle character over a long range of isotopes (isotones). This is because such levels do not mix with neighboring normal-parity levels. Therefore, one observes rather similar $E2$ energies above $11/2^-$ levels in Pd isotopes, characteristic of a decoupled band, which indicate moderate deformation of $11/2^-$ levels in $^{103-117}$Pd isotopes.

In contrast, various orbitals of positive parity are populated with an increasing neutron number, which may interact with each other and produce more collective states. In this way the
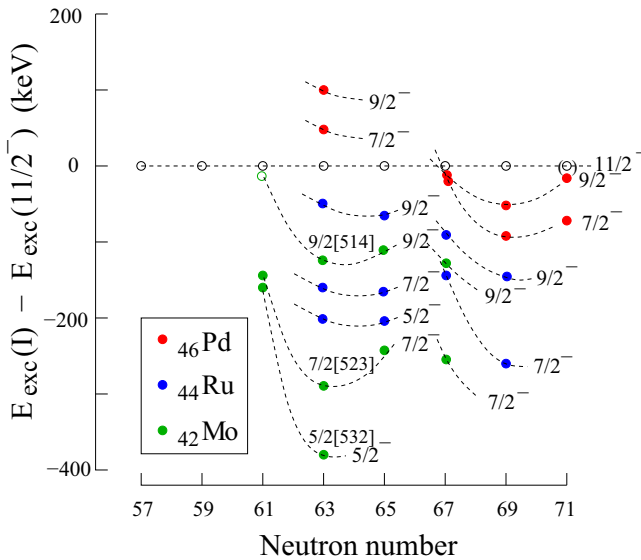
FIG. 8. Systematics of negative-parity levels in odd-A Mo, Ru, and Pd isotopes. The data are taken from Refs. [46–51] and the present work. Dashed lines are drawn to guide the eye.

$5/2^+$ ground states in palladium will increase its deformation with the growing neutron number. The resulting increasing difference in the deformation between the $11/2^-$ isomer and the ground state in $^{107-111}$Pd will result in increasing hindrance factor in $^{107-111}$Pd isotopes.

At still higher neutron number, in ^{113,115}Pd isotopes the hindrance factor decreases, suggesting smaller difference between shapes of the isomer and the ground state. This is most evident in ^{115}Pd. Here the ground state has spin $1/2^+$ [7], which is probably due to the less deformed $\nu d_{3/2}$ shell. On the other hand the isomeric state most likely gains some deformation. Such an increase is supported by the observed lowering of quadrupole-transition energy in bands on top of the $11/2^-$ levels in ^{113,115}Pd. Another indication of an increasing deformation of negative-parity states in the two isotopes is the lower spin of the isomeric level.

This latter effect is supported by the systematics of negative-parity excitations in odd-A Mo, Ru, and Pd isotopes, shown in Fig. 8. We note that the new $7/2^-$ spin-parity of the isomer in ^{117}Pd makes the systematic trends for Pd isotopes similar to the trends for Mo and Ru isotopes. It surpasses previous ones [7,8] partly incorrect due to the incomplete or wrong data available at that time. As already discussed in Ref. [7] the parabolic trends results from filling the subsequent 5/2[532], 7/2[523], etc., orbitals with nucleons, as the Fermi level goes up. At $61 \leqslant N \leqslant 65$ the 5/2[532] orbital is populated. When this orbital is full, the 7/2[523] orbital is filled at $67 \leqslant N \leqslant 71$. In spherical and weakly deformed nuclei the $11/2^-$ level will have the highest energy. With increasing deformation the 5/2[532], 7/2[523], and 9/2[514] levels will drop below the 11/2 level. This is illustrated in Fig. 8 where, for example, the $5/2^-$ ground state of ^{105}Mo$_{63}$, which is well deformed with a strongly coupled band on top of it [21] is well below the $11/2^-$ level. Analogously, a strongly coupled band is observed on top of the $7/2^-$ level at 222.2 keV in

^{109}Mo$_{67}$ [22]. Therefore, the lowering of the $7/2^-$ level below the $11/2^-$ level in $^{113-117}$Pd isotopes is a sign of an increasing deformation of the negative-parity system in these nuclei.

We note that the improved systematics, shown in Fig. 8, suggest positions of $7/2^-$ and $9/2^-$ levels in ^{111}Pd approximately 40 keV and 80 keV above the $11/2^-$ isomer at 172.2 keV. It is of interest to search for these excitations in order to verify the proposed picture. We note that both levels are expected to be populated in β decay of the $7/2^+$ g.s. of ^{111}Rh, similarly to what is observed in ^{117}Pd and ^{109}Pd [52]. Interestingly, a $(7/2^-)$ excitation was proposed in ^{111}Pd at 191.3(3) keV in Ref. [58], but was not adopted by evaluators [48].

C. Properties of states and deformations in ^{117}Pd

In many theoretical works [2,40,59–61], two potential minima for a prolate and an oblate shape, as well as a triaxial shape, are predicted in the palladium nuclei in the $A = 110–120$ region. The potential energy curves calculated in Ref. [59] show two minima for even-even palladium isotopes from $A = 114$ to $A = 118$. Prolate-type deformation is predicted for ground states and an oblate-type for the isomers in Pd isotopes [59,60]. Deformed shell-model calculations for even-even palladium isotopes [1] predict quadrupole deformation with $\beta_2 > 0.2$.

In ^{115}Pd we have proposed spin $1/2^+$ for the ground state [7]. The $1/2^+$ excitation may be formed in both prolate and oblate minima of the nuclear potential in Pd isotopes. In Fig. 6 one observes the $1/2_1^+$ excitation close to the Fermi surface in the whole range $^{103-117}$Pd. It is obvious that this excitation must correspond to various configurations.

At the low-neutron side, in spherical $^{103-107}$Pd isotopes it probably corresponds to the $\nu 3s_{1/2}$ single-particle configuration. In $^{109-113}$Pd the $1/2_1^+$ level is most likely due to the 1/2[400] orbital (in ^{113}Pd this is the $1/2_2^+$ experimental level). Finally, in $^{113-117}$Pd the 1/2[440] orbital in the oblate minimum is probably responsible for the $1/2_1^+$ excitation, which forms ground states in ^{115}Pd and ^{117}Pd. Therefore, in ^{115}Pd the $E3$ transition between the weakly deformed $7/2^-$ oblate isomer and the $1/2^+$ ground state of like deformation has relatively low hindrance of 497 only. In ^{117}Pd two $3/2^+$ levels, which probably correspond to the 3/2[402] orbital in the interacting prolate and oblate minima, appear at 34.6 and 131.7 keV, enabling $M2$ decays from the $7/2^-$ oblate isomer. The admixture of the prolate shape increases moderately the hindrance factor.

Excited levels in ^{117}Pd, populated by β^- decay of ^{117}Rh, can be divided into three groups, marked in Fig. 4 with capital letters A, B, and C, according to their decay preferences. The levels at 207.7 and 225.4 keV (from group C in Fig. 4) decay preferably to the ground state. The 17.8-keV transition indicates similar structure of both levels. Because of the oblate nature of the ground state, proposed above, they are also candidates for an oblate deformation. Other levels from group C, decaying to the 207.7- and 225.4-keV levels are probably oblate, as well.

Levels from group A do not communicate with levels from group C. Therefore, we propose that their structure is dominated by prolate deformation. Some admixture of oblate

shape is likely because these levels are related to the two $3/2^+$ levels 34.6 and 131.7 keV, proposed to be mixed. Here the 236.7- and 321.2-keV levels are likely the beginning of a rotational band corresponding to the 5/2[402] configuration, though again with possible admixture of an oblate deformation, as discussed in Sec. V A. We note that this $5/2^+$ band in ^{117}Pd is not well developed. In particular one might expect the population of the $9/2^+$ member of this band in β decay of the $7/2^+$ parent as observed in ^{113}Pd. A possible explanation of different populations is that in ^{113}Pd the $5/2^+$ ground-state band is populated strongly because the $7/2^+$ g.s. of ^{113}Rh is prolate, while in ^{115}Pd and ^{117}Pd it is populated weakly because the $7/2^+$ g.s. of ^{115,117}Rh are triaxial or oblate.

Levels from group B in Fig. 4 decay to all, the oblate levels C, the mixed $3/2_1^+$, 34.6-keV and $3/2_2^+$, 131.7-keV levels and the prolate 236.7-keV level but not directly to the ground state. This suggests a difference in deformation and we propose that levels from group B correspond to a triaxial shape. High β feeding of the 516.5-keV level in group B may be explained if the 516.5-keV level has a similar deformation as the $7/2^+$ ground state of ^{117}Rh.

Summarizing, we propose that the triaxially deformed ^{117}Rh ground state (see Sec. IV A), decays to the three groups of levels in ^{117}Pd, which have predominantly prolate (A), triaxial (B), and oblate (C) deformation. The $3/2_1^+$, 34.6-keV and $3/2_2^+$, 131.7-keV levels are probably due to interacting prolate and oblate solutions.

VI. STRENGTH DISTRIBUTION IN β DECAY

In very neutron-rich isotopes the β-decay rates competing with the neutron-capture cross sections define the course of the r-process path. The third element in this picture is the nuclear deformation, which generally should stabilize nuclei and shift the path further away from the stability line, as argued in Ref. [5]. The new region of oblate deformation above $N = 70$, discussed in previous sections would be consistent with the expectation that the r-process path reaches the $N = 82$ shell closure at $Z \approx 45$ [62]. In this section we will verify the information on the β^--decay rates in this region, especially on the fast, allowed transitions.

We have determined the experimental Gamow-Teller transition strengths $B_i(GT)$ for the β^- decay of the ground states of ^{115}Rh and ^{117}Rh isotopes by using the comparative half-lives $f_i t_i$ measured for the observed β transitions. Summing up the $B_i(GT)$ over all transitions in a decay of the nucleus of interest we obtained the total $B(GT)$ value

$$\Sigma B(GT) = \sum_i B_i(GT) = \sum_i \frac{3860}{f_i t_i}.$$

The distributions of $B_i(GT)$ values are presented in Fig. 9 for the decays of $A = 115$ and 117 rhodium nuclei. One observes a similar pattern of $B_i(GT)$ distributions in the two decays of rhodium to palladium, with most of the intensity below 800 keV. The total $B(GT)$ values of 0.13 and 0.12, shown in Fig. 9, are also very similar.

In β decay of rhodium the low-lying levels in palladium are single-neutron states and the higher-energy states contain a single neutron and two unpaired protons. The $B_i(GT)$
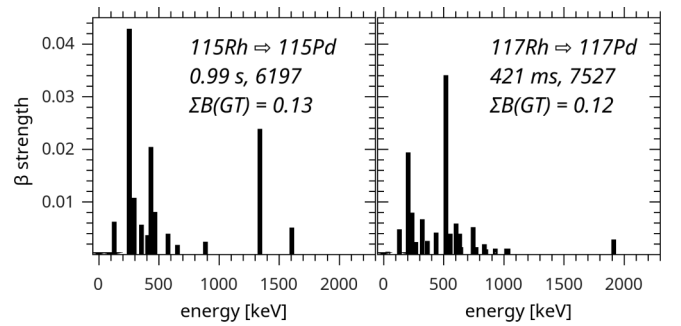

FIG. 9. The distributions of $B(GT)$ decay strength for odd $A = 115$ and 117 ground-state decays of rhodium to palladium. The data are taken from Ref. [7] and this work. The half-lives [36], the beta-decay energies in keV [35] and the total $B(GT)$ strengths observed in this work are shown also.

distributions in Fig. 9 suggest that the β decay of rhodium preferably populates single-particle states. In preparation there are results on β decay of ^{117}Pd to ^{117}Ag, where we observe, in the same experiment and with the same detector setup, most of the $B(GT)$ strength going to three quasiparticle states.

VII. SUMMARY

The present work reports studies of β^- decay of monoisotopic samples of ^{117}Rh, which populated excited states in ^{117}Pd. Arguments in favor of the $7/2^+$ spin parity for the ground state of ^{117}Rh have been presented. 53 new transitions and 23 new levels were proposed in the excitation scheme of ^{117}Pd. Based on the observed population in β^- decay, a new spin parity of $7/2^-$ has been proposed for the 19.1 ms isomer at 203.2 keV in ^{117}Pd, leading to the new spin parity of $1/2^+$ for the ground state of ^{117}Pd. We also proposed that the $11/2^-$ level in ^{117}Pd is located no more than 20 keV above the 266.5-keV level (see Fig. 8), to which a new spin parity $9/2^-$ has been assigned.

The $1/2^+$ ground-state spin in ^{115,117}Pd (and in their isotones ^{113,115}Ru [24,26]), in contrast to the $5/2^+$ ground-state spin in lighter palladium and ruthenium isotopes, and significantly more low-energy excitations in ^{117}Pd, as compared to lighter Pd isotopes, indicate the appearance of new deformed structures above the neutron number $N = 67$. We propose that the new states correspond to configurations with oblate deformation, which appear in addition to the prolate-deformed structures observed in the lighter isotopes. In ^{117}Pd there are also new levels due to mixing of the two deformations and due to a triaxial deformation. The observed β decays of ^{117}Rh suggest that as the ground state of ^{117}Rh has a triaxial deformation, its decay populates levels of all, the prolate, oblate, and triaxial shapes in ^{117}Pd.

The new data allows a consistent explanation of the exceptional evolution of hindrance factors of the isomeric transitions in $^{103-117}$Pd, as due to changes in the deformation of the isomeric levels from spherical to weakly oblate deformed vs. changes of levels they decay to, from spherical to prolate deformed and to weakly oblate deformed. With new data in favor of the transition to an oblate shape expected past the middle of the $50 < N < 82$ neutron shell the present work provides a demanding case for testing nuclear models.

[1] S. Lalkovski, A. M. Bruce, A. M. D. Bacelar, M. Górska, S. Pietri, Z. Podolyák, P. Bednarczyk, L. Caceres, E. Casarejos, I. J. Cullen *et al.*, Phys. Rev. C **88**, 024302 (2013).

[2] J. Skalski, S. Mizutori, and W. Nazarewicz, Nucl. Phys. A **617**, 282 (1997).

[3] F. R. Xu, P. M. Walker, and R. Wyss, Phys. Rev. C **65**, 021303 (2002).

[4] W. Urban, T. Rząca-Urban, J. L. Durell, W. R. Phillips, A. G. Smith, B. J. Varley, I. Ahmad, and N. Schulz, Eur. Phys. J. A **20**, 381 (2004).

[5] W. Urban, T. Rząca-Urban, J. L. Durell, A. G. Smith, and I. Ahmad, Eur. Phys. J. A **24**, 161 (2005).

[6] J. Kurpeta, W. Urban, A. Płochocki, J. Rissanen, J. A. Pinston, V.-V. Elomaa, T. Eronen, J. Hakala, A. Jokinen, A. Kankainen *et al.*, Phys. Rev. C **84**, 044304 (2011).

[7] J. Kurpeta, W. Urban, A. Płochocki, J. Rissanen, V.-V. Elomaa, T. Eronen, J. Hakala, A. Jokinen, A. Kankainen, P. Karvonen *et al.*, Phys. Rev. C **82**, 027306 (2010).

[8] W. Urban, A. Złomaniec, G. Simpson, J. A. Pinston, J. Kurpeta, T. Rząca-Urban, J. L. Durell, A. G. Smith, B. J. Varley, N. Schulz *et al.*, Eur. Phys. J. A **22**, 157 (2004).

[9] D. Fong, J. K. Hwang, A. V. Ramayya, J. H. Hamilton, Y. X. Luo, P. M. Gore, E. F. Jones, W. B. Walters, J. O. Rasmussen, M. A. Stoyer *et al.*, Phys. Rev. C **72**, 014315 (2005).

[10] H. Penttilä, P. P. Jauho, J. Äystö, P. Decrock, P. Dendooven, M. Huyse, G. Reusen, P. VanDuppen, and J. Wauters, Phys. Rev. C **44**, R935(R) (1991).

[11] H. Penttilä, J. Äystö, K. Eskola, Z. Janas, P. Jauho, A. Jokinen, M. Leino, J. Parmonen, and P. Taskinen, Z. Phys. A **338**, 291 (1991).

[12] H. Penttilä, Ph.D. thesis, Dept. of Physics, University of Jyväskylä, Research Report 1/1992, 1992 (unpublished).

[13] H. Penttilä, T. Enqvist, P. Jauho, A. Jokinen, M. Leino, J. Parmonen, J. Äystö, and K. Eskola, Nucl. Phys. A **561**, 416 (1993).

[14] J. Shannon, W. Phillips, J. Durell, B. Varley, W. Urban, C. Pearson, I. Ahmad, C. Lister, L. Morss, K. Nash *et al.*, Phys. Lett. B **336**, 136 (1994).

[15] A. Guessous, N. Schulz, W. Phillips, I. Ahmad, M. Bentaleb, J. Durell, M. Jones, C. Pearson, M. Leddy, E. Lubkiewicz *et al.*, Phys. Rev. Lett. **75**, 2280 (1995).

[16] A. Guessous, N. Schulz, M. Bentaleb, E. Lubkiewicz, J. Durell, C. Pearson, W. Phillips, J. Shannon, W. Urban, B. Varley *et al.*, Phys. Rev. C **53**, 1191 (1996).

[17] W. Urban, T. Rząca-Urban, J. L. Durell, A. G. Smith, and I. Ahmad, Phys. Rev. C **70**, 057308 (2004).

[18] C. Droste, S. G. Rohoziński, L. Próchniak, K. Zając, W. Urban, J. Srebrny, and T. Morek, Eur. Phys. J. A **22**, 179 (2004).

[19] W. Urban, T. Rząca-Urban, C. Droste, S. G. Rohoziński, J. L. Durell, W. R. Phillips, A. G. Smith, B. J. Varley, N. Schulz, I. Ahmad *et al.*, Eur. Phys. J. A **22**, 231 (2004).

[20] W. Urban, T. Rząca-Urban, J. A. Pinston, J. L. Durell, W. R. Phillips, A. G. Smith, B. J. Varley, I. Ahmad, and N. Schulz, Phys. Rev. C **72**, 027302 (2005).

[21] J. A. Pinston, W. Urban, C. Droste, T. Rząca-Urban, J. Genevey, G. S. Simpson, J. L. Durell, A. G. Smith, B. J. Varley, and I. Ahmad, Phys Rev. C **74**, 064304 (2006).

[22] W. Urban, C. Droste, T. Rząca-Urban, A. Złomaniec, J. L. Durell, A. G. Smith, B. J. Varley, and I. Ahmad, Phys. Rev. C **73**, 037302 (2006).

[23] J. Kurpeta, V.-V. Elomaa, T. Eronen, J. Hakala, A. Jokinen, P. Karvonen, I. D. Moore, H. Penttilä, A. Płochocki, S. Rahaman *et al.*, Eur. Phys. J. A **31**, 263 (2007).

[24] J. Kurpeta, W. Urban, C. Droste, A. Płochocki, S. G. Rohoziński, T. Rząca-Urban, T. Morek, L. Próchniak, K. Starosta, J. Äystö *et al.*, Eur. Phys. J. A **33**, 307 (2007).

[25] W. Urban, J. A. Pinston, T. Rząca-Urban, J. Kurpeta, A. G. Smith, and I. Ahmad, Phys. Rev. C **82**, 064308 (2010).

[26] J. Kurpeta, J. Rissanen, A. Płochocki, W. Urban, V.-V. Elomaa, T. Eronen, J. Hakala, A. Jokinen, A. Kankainen, P. Karvonen *et al.*, Phys. Rev. C **82**, 064318 (2010).

[27] J. Rissanen, J. Kurpeta, A. Płochocki, V.-V. Elomaa, T. Eronen, J. Hakala, A. Jokinen, A. Kankainen, P. Karvonen, I. D. Moore *et al.*, Eur. Phys. J. A **47**, 97 (2011).

[28] D. Kameda, T. Kubo, T. Ohnishi, K. Kusaka, A. Yoshida, K. Yoshida, M. Ohtake, N. Fukuda, H. Takeda, K. Tanaka *et al.*, Phys. Rev. C **86**, 054319 (2012).

[29] J. Marcellino, E. H. Wang, C. J. Zachary, J. H. Hamilton, A. V. Ramayya, G. H. Bhat, J. A. Sheikh, A. C. Dai, W. Y. Liang, F. R. Xu *et al.*, Phys. Rev. C **96**, 034319 (2017).

[30] I. Moore, T. Eronen, D. Gorelov, J. Hakala, A. Jokinen, A. Kankainen, V. Kolhinen, J. Koponen, H. Penttilä, I. Pohjalainen *et al.*, Nucl. Instrum. Meth. Phys. Res. B **317**, 208 (2013).

[31] A. Nieminen, J. Huikari, A. Jokinen, J. A. P. Campbell, and E. Cochrane, Nucl. Instrum. Methods Phys. Res., Sect. B **469**, 244 (2001).

[32] T. Eronen, V. S. Kolhinen, V.-V. Elomaa, D. Gorelov, U. Hager, J. Hakala, A. Jokinen, A. Kankainen, P. Karvonen, S. Kopecky *et al.*, Eur. Phys. J. A **48**, 46 (2012).

[33] V. S. Kolhinen, T. Eronen, D. Gorelov, J. Hakala, A. Jokinen, K. Jokiranta, A. Kankainen, M. Koikkalainen, J. Koponen, H. Kulmala *et al.*, Nucl. Instrum. Meth. Phys. Res. B **317**, 506 (2013).

[34] F. Montes, A. Estrade, P. T. Hosmer, S. N. Liddick, P. F. Mantica, A. C. Morton, W. F. Mueller, M. Ouellette, E. Pellegrini, P. Santi *et al.*, Phys. Rev. C **73**, 035801 (2006).

[35] M. Wang, G. Audi, F. Kondev, W. Huang, S. Naimi, and X. Xu, Chin. Phys. C **41**, 030003 (2017).

[36] G. Audi, F. Kondev, M. Wang, W. Huang, and S. Naimi, Chin. Phys. C **41**, 030001 (2017).

[37] T. Kibédi, T. Burrows, M. Trzhaskovskaya, P. Davidson, and C. Nestor Jr., Nucl. Instrum. Methods Phys. Res., Sect. A **589**, 202 (2008).

[38] S. H. Liu, J. H. Hamilton, A. V. Ramayya, A. Gelberg, L. Gu, E. Y. Yeoh, S. J. Zhu, N. T. Brewer, J. K. Hwang, Y. X. Luo *et al.*, Phys. Rev. C **84**, 014304 (2011).

[39] A. Navin, M. Rejmund, S. Bhattacharyya, R. Palit, G. H. Bhat, J. A. Sheikh, A. Lemasson, S. Bhattacharya, M. Caamaño, E. Clément *et al.*, Phys. Lett. B **767**, 480 (2017).

[40] P. Möller, A. J. Sierk, R. Bengtsson, H. Sagawa, and T. Ichikawa, At. Data Nucl. Data Tables **98**, 149 (2012).

[41] W. Y. Liang, C. F. Jiao, F. R. Xu, and X. M. Fu, Sci. China Phys. Mech. Astron. **59**, 692012 (2016).

[42] G. Lhersonneau, B. Pfeiffer, J. Alstad, P. Dendooven, K. Eberhardt, S. Hankonen, I. Klockl, K.-L. Kratz, A. Nahler, R. Malmbeck *et al.*, Eur. Phys. J. A **1**, 285 (1998).

[43] Evaluated Nuclear Structure Data File (J. Blachot, ^{101}Rh, cutoff date July 2006), http://www.nndc.bnl.gov/ensdf.

[44] D. De Frenne, Nucl. Data Sheets **110**, 2081 (2009).

[45] D. De Frenne and E. Jacob, Nucl. Data Sheets **105**, 775 (2005).

[46] J. Blachot, Nucl. Data Sheets **109**, 1383 (2008).

[47] S. Kumar, J. Chen, and F. G. Kondev, Nucl. Data Sheets **137**, 1 (2016).

[48] J. Blachot, Nucl. Data Sheets **110**, 1239 (2009).

[49] J. Blachot, Nucl. Data Sheets **111**, 1471 (2010).

[50] J. Blachot, Nucl. Data Sheets **113**, 2391 (2012).

[51] Evaluated Nuclear Structure Data File (J. Blachot, ^{117}Rh, ^{117}Pd, cutoff date March 2009), http://www.nndc.bnl.gov/ensdf.

[52] B. Bucher, H. Mach, A. Aprahamian, G. S. Simpson, J. Rissanen, D. G. Ghiţă, B. Olaizola, W. Kurcewicz, J. Äystö, I. Bentley *et al.*, Phys. Rev. C **92**, 064312 (2015).

[53] Y. X. Luo, S. C. Wu, J. Gilat, J. O. Rasmussen, J. H. Hamilton, A. V. Ramayya, J. K. Hwang, C. J. Beyer, S. J. Zhu, J. Kormicki *et al.*, Phys. Rev. C **69**, 024315 (2004).

[54] T. Venkova, M.-G. Porquet, I. Deloncle, B. J. P. Gall, H. D. Witte, P. Petkov, A. Bauchet, T. Kutsarova, E. Gueorgieva, J. Duprat *et al.*, Eur. Phys. J. A **6**, 405 (1999).

[55] H. Penttilä, J. Äystö, P. Jauho, A. Jokinen, J. M. Parmonen, P. Taskinen, K. Eskola, M. Leino, P. Dendooven, and C. N. Davids, Phys. Scr. **T32**, 38 (1990).

[56] J. Kurpeta, W. Urban, A. Płochocki, T. Rząca-Urban, A. G. Smith, J. F. Smith, G. S. Simpson, I. Ahmad, J. P. Greene, A. Jokinen *et al.*, Phys. Rev. C **90**, 064315 (2014).

[57] P. M. Endt, At. Data Nucl. Data Tables **26**, 47 (1981).

[58] N. Kaffrell, H. Tetzlaff, N. Trautmann, P. Hill, S. Hoglund, G. Skarnemark, J. Alstad, P. Gelder, E. Jacobs, K. Wolfsberg *et al.*, in *Jahresbericht 1983* (Inst. fur Kernchemie, Univ. Mainz, 1984), p. 62.

[59] P. Sarriguren, Phys. Rev. C **91**, 044304 (2015).

[60] M. Bhuyan, Phys. Rev. C **92**, 034323 (2015).

[61] P. Möller, A. J. Sierk, T. Ichikawa, and H. Sagawa, At. Data Nucl. Data Tables **109-110**, 1 (2016).

[62] G. Lorusso, S. Nishimura, Z. Y. Xu, A. Jungclaus, Y. Shimizu, G. S. Simpson, P.-A. Söderström, H. Watanabe, F. Browne, P. Doornenbal *et al.*, Phys. Rev. Lett. **114**, 192501 (2015).